Molecular Biology of the Cell
Vol. 8, 421–430, March 1997

Modification of Cys-837 Identifies an Actin-binding Site in the β-Propeller Protein Scruin

Shujun Sun,*† Matthew Footer,* and Paul Matsudaira‡

*Whitehead Institute for Biomedical Research, and ‡Department of Biology, Massachusetts Institute of Technology, Cambridge, Massachusetts 02142

Submitted September 29, 1996; Accepted December 26, 1996
Monitoring Editor: J. Richard McIntosh

In the acrosomal process of *Limulus* sperm, the β-propeller protein scruin cross-links actin into a crystalline bundle. To confirm that scruin has the topology of a β-propeller protein and to understand how scruin binds actin, we compared the solvent accessibility of cysteine residues in scruin and the acrosomal process by chemical modification with (1,5-IAEDANS). In soluble scruin, the two most reactive cysteines of soluble scruin are C837 and C900, whereas C146, C333, and C683 are moderately reactive. This pattern of reactivity is consistent with the topology of a typical β-propeller protein; all of the reactive cysteines map to putative loops and turns whereas the unreactive cysteines lie within the predicted interior of the protein. The chemical reactivities of cysteine in the acrosomal process implicate C837 at an actin-binding site. In contrast to soluble scruin, in the acrosomal process, C837 is completely unreactive while the other cysteines become less reactive. Binding studies of chemically modified scruin correlate the extent of modification at C837 with the extent of inhibition of actin binding. Furthermore, peptides corresponding to residues flanking C837 bind actin and narrow a possible actin-binding region to a KQK sequence. On the basis of these studies, our results suggest that an actin-binding site lies in the C-terminal domain of scruin and involves a putative loop defined by C837.

INTRODUCTION

An unusual structure, a coiled actin bundle, surrounds the base of the nucleus in an unactivated *Limulus* sperm (André, 1965; Tilney, 1975). The actin coil is not a smooth circle but is segmented into arms (straight segments) connected by elbows (bends) (De Rosier and Tilney, 1984). At fertilization, the bundle uncoils into a straight crystalline bundle, the acrosomal process, that extends for 80 μm from the head of the sperm (Tilney, 1975). As it converts from the coiled to straight form, the actin filaments slip past one another and untwist by 0.2 degree per subunit (De Rosier and Tilney, 1984). This dynamic rearrangement of actin must be dependent on scruin, the only actin cross-linking protein in the bundle. Understanding how scruin organizes actin before and after sperm activation can provide insight into the mechanism that generates the force needed to straighten and extend the bundle.

The first views into scruin structure and the interaction between scruin and actin are provided by cryo-electron microscopy. In ice, the actin bundle is crystalline and diffracts to better than 5 Å (Schmid *et al.*, 1994). A 15-Å helical reconstruction of a single filament from the bundle shows that scruin decorates the outside of an actin filament, and scruin itself is shaped like a dumbbell that lies across the filament axis (Owen and DeRosier, 1993; Schmid *et al.*, 1994). The two domains, one spherical and the other elongated, are roughly equal in size and bind to separate actin subunits on the same filament. Based on sequence and limited proteolysis experiments, the domains are homologous and protease resistant (Way *et al.*, 1995a). A protease-sensitive neck region between the domains is highly helical and binds calmodulin, an obligate subunit that may modulate scruin–actin interactions during the acrosome reaction (Sanders *et al.*, 1996).

† Corresponding author: Whitehead Institute for Biomedical Research, Massachusetts Institute of Technology, Nine Cambridge Center, Cambridge, Massachusetts 02142.

© 1997 by The American Society for Cell Biology

Closer examination of the model surprisingly reveals where scruin binds actin. Despite their homology, the domains bind to different rather than identical actin subdomains. The elongated domain sits on the face of actin subdomain 3, and the spherical domain overlays the back of subdomain 1. The putative binding sites on actin are homologous helix-loop strand motifs exposed at the interface between actin and the scruin domains (Schmid *et al.*, 1994). Homologous domains would be expected to have identical binding sites but scruin may have taken advantage of the internal homology in actin to find equivalent binding sites.

Although electron microscopic (EM) reconstructions are limited to 15-Å resolution, a more detailed understanding of scruin structure is made possible by its similarity with a superfamily of proteins that are organized around a β-propeller motif. Protein sequence analysis shows that each domain of scruin contains a 50-residue sequence that is repeated six times. X-ray crystallographic studies of galactose oxidase (Ito *et al.*, 1994), the sialidase family of proteins (Bork and Doolittle, 1994), and the WD-40 repeat proteins such as the β-subunit of G proteins (Wall *et al.*, 1995) show that the repeat sequence represents a four-stranded antiparallel β-sheet twisted like a blade of a propeller. In galactose oxidase, seven blades are joined by loops of variable lengths to form a disk-shaped structure with a central water-filled channel. Although the number of β-propellers can be two to eight, depending on the protein, a consistent feature of these proteins is that the outermost strand (strand 4) in the sheet and all of the connecting loops and turns contribute most of the residues to the surface of the protein. Based on the sequence homologies and three-dimensional (3D) structures of the known β-propeller proteins, we have proposed that the six repeats in both N- and C-terminal domains in scruin are also organized into a six-bladed β-propeller structure connected by a short α-helical region (Sanders *et al.*, 1996).

Although we have insight into scruin structure and its interactions with actin, we do not know where actin binds scruin and how scruin organizes actin into a bundle. In our model, the actin-binding sites on scruin must involve the exposed surface of scruin. In this article, we use a classic biochemical approach, modification of cysteine residues, to probe the surface of scruin and to identify sites that are protected from modification by actin binding. Our experiments suggest two conclusions: 1) The topology of scruin predicted from the 3D structures of β-propeller proteins is confirmed by the pattern of chemical reactivity. 2) An actin-binding site lies in the C-terminal domain of scruin and must involve a loop defined by C837. These findings strengthen our understanding of scruin structure and, to our knowledge, for the first time provide insight into how scruin binds actin. Furthermore, our studies on scruin–actin interactions may provide important clues as to how other β-propeller proteins with putative cytoskeletal functions like kelch in the ring canal of oocyte may interact with actin.

MATERIALS AND METHODS

Materials

ATP, 5,5′-dithiobis-(2-nitrobenzoic acid) (DTNB), and protease inhibitors (pepstatin A, leupeptin, aprotinin, benzamidine, and phenylmethylsulfonyl fluoride) were purchased from Sigma (St. Louis, MO). Methyl-6-(*N*-heptylcarbamoyl)-α-D-glucopyranoside (HECAMEG) was purchased from Calbiochem (San Diego, CA). 5-({[(2-Iodoacetyl)amino]ethyl}amino)naphthalene-1-sulfonic acid (1,5-IAEDANS) was purchased from Molecular Probes (Eugene, OR). Artificial sea water was purchased from Tropic Marin (Warterberg, Germany). Sequencing grade trypsin was obtained from Boehringer Mannheim (Indianapolis, IN).

Purification of True Discharge and Scruin

The true discharge form of the acrosomal process and scruin were purified from *Limulus* sperm (Sanders *et al.*, 1996). The yield of the protocol was increased 10–15-fold. In the modified protocol, 20 ml of sperm were collected from healthy horse shoe crabs and activated by mixing with 200 ml of 25 mM $CaCl_2$ in 0.2 g/ml artificial sea water containing a mixture of protease inhibitors (0.5 mg/ml phenylmethylsulfonyl fluoride, 0.75 mg/ml benzamidine, 10 μg/ml pepstatin A, 10 μg/ml leupeptin, 1 TIU/ml aprotinin). After 15 min on ice, the activated sperm were sheared four times through a 21-gauge needle and then centrifuged at 4000 rpm in an SS-34 rotor for 10 min to separate the acrosomes (supernatant) from the sperm heads (pellet). The pellet was resuspended in 200 ml of 25 mM $CaCl_2$ in 0.2 g/ml sea water and centrifuged. The supernatants were combined and centrifuged at 19,000 rpm for 15 min to pellet the acrosomes. To remove the plasma membrane, the acrosomes were resuspended in 30 ml of 20 mM detergent HECAMEG in buffer A [0.1 M NaCl, 1 mM $CaCl_2$, 1 mM dithiothreitol (DTT), 0.01% NaN_3, 10 mM Tris, pH 8.0]. The demembranated acrosomes were collected by centrifugation for 15 min at 19,000 rpm and washed once with HECAMEG in buffer A and then three times with 40 ml of buffer A. The purity of the actin bundle was checked by SDS-PAGE. In this preparation, 10–15 mg of acrosomal process could be isolated from 20 ml of *Limulus* sperm.

To purify scruin, the true discharges were suspended with 5 ml of buffer A and mixed with an equal volume of 2 M $CaCl_2$. The turbid suspension of actin bundles immediately cleared, indicating that the actin bundle was disrupted. The actin filaments were separated from the scruin–calmodulin complex by centrifugation at 100,000 rpm in a TLA 100 rotor. The supernatant was passed through a Qiagen-5 column to remove DNA and then chromatographed through a Sephacyl S200 HR gel filtration column equilibrated in buffer A. Fractions containing scruin were pooled and then purified from minor contaminants on a 1-ml HiTrap-Q ion exchange fast-performance liquid chromatography column (Pharmacia, Uppsala, Sweden). The protein concentration of the scruin–calmodulin complex was determined by using the Bradford assay. In a standard preparation, 4–7 mg of scruin–calmodulin complex were purified from the 20 ml of sperm.

Calmodulin was separated from the scruin–calmodulin complex by heating the mixture at 90°C for 15 min and then renaturing calmodulin at room temperature for 30 min. The mixture was centrifuged to remove precipitated scruin. The purity of calmodulin was checked by SDS-PAGE.

Titration of Reactive Cysteines of Scruin

Scruin was reduced with 1 mM DTT and dialyzed against 2 mM EDTA and 0.1 M Tris (pH 7.5). Ellman's reagent, DTNB, was added

to 5 μM scruin in a cuvette at final molar ratios of DTNB to scruin of 1.5:1, 3:1, 6:1, and 41:1. The production of 5-thio-2-nitrobenzoic acid (TNB) was measured at 410 nm (ϵ_{410} nm = 13,600 $cm^{-1} \cdot M^{-1}$) with a Aviv 118 DS UV-Vis spectrophotometer.

Actin-binding Assay and Electron Microscopy

Reconstitution of scruin-actin bundle was performed with scruin modified with 1,5-IAEDANS and rabbit skeletal actin. Unmodified scruin was used as a control. The labeled and unlabeled scruin were dialyzed against actin-binding buffer [50 mM NaCl, 1 mM $MgCl_2$, 0.1 mM ethylene glycol-bis(β-aminoethyl ether)-*N,N,N',N'*-tetraacetic acid, 0.5 mM ATP, 10 mM piperazine-*N,N'*-bis(2-ethanesulfonic acid), pH 7.0] for 3 h and then mixed in a 1:1 M ratio with filamentous actin (f-actin; 5 μM) in binding buffer (total volume 50 μl). After 1 h at room temperature, a 3-μl aliquot was taken for EM examination and a 7-μl aliquot was saved for SDS-PAGE analysis. The remaining sample (40 μl) was centrifuged at 100,000 rpm for 15 min (TLA 100, Beckman, Fullerton, CA). Supernatants and pellets (resuspended in equal volume with the supernatant) were analyzed by SDS-PAGE. For EM analysis, samples were applied onto a carbon film, negatively stained with 1% uranyl acetate, and examined in a Phillips 410 electron microscope at 80 kV.

Mapping Reactive Cysteines on Scruin and on the Scruin-Actin Bundle

Purified scruin–calmodulin complex and the true discharge were dialyzed against degassed buffer B (0.1 M NaCl, 1 mM $CaCl_2$, 50 mM Tris, pH 8.0) for 3 h at 4°C. After dialysis, the samples were mixed with 1,5-IAEDANS at dye:scruin molar ratios of 1:1 6:1, 13:1, and 45:1 and then incubated at 4°C for 18 h. Unreacted 1,5-IAEDANS was removed by dialysis, and the concentration of modified proteins was measured by using the Bradford protein assay. The dye-modified scruin and true discharge were completely digested by sequence grade trypsin at 37°C for 24 h. The digest peptides were separated by high-performance liquid chromatography (HPLC) through a Vydac C_{18} column of 2.1 × 25 mm, with monitoring at 214 nm for peptides and 335 nm for 1,5-IAEDANS. Fractions containing modified peptides were further purified on a C_{18} Vydac column of 1 × 25 mm. To quantify the amount of each labeled peptide, the peak areas were calculated and compared with peaks from injections of 1,5-IAEDANS chromatographed through the same column. The purity and the molecular weight of the labeled peptides were confirmed by matrix-assisted laser desorption time-of-flight mass spectrometry in a PerSeptive Biosystems Voyager Elite mass spectrometer (PerSeptive Biosystem, Framingham, MA). Peptides containing the reactive cysteines were further identified by peptide sequencing in an Applied Biosystems model 475A sequencer (Foster City, CA).

Peptide-binding Assay

Four peptides were synthesized (Biosynthesis, Lewisville, TX) and purified by HPLC. Peptide M39 corresponds to residues 830–842 of scruin. The sequence was chosen to flank the reactive cysteine C837 of scruin and to lie within a putative loop in a model of a β-propeller protein. Peptide M39R2 is a random sequence of M39. Peptide M39R3 and M39R4 are derived from M39 by replacing the cysteine with alanine and adding cysteine to the N- (M39R3) or the C- (M39R4) terminal end of the peptides. The sequences of these peptides are as follows: M39, **KQK**TSLGCPRHSA; M39R2, SAKHGLKTPCSQR; M39R3, C**KQK**TSLGAPRHSA; M39R4, **KQK**TSLGAPRHSAC. Peptide dimers (disulfide bond) were formed by incubating the peptide at room temperature for at least 24 h, and the dimer formation was checked by mass spectrometry and HPLC. The actin bundling activities of each peptide dimer were determined by using an Hitachi F-4500 fluorometer by monitoring 90-degree light scattering (excitation and emission of 550 nm) of f-actin (3 μM) mixed with various amounts of peptide. Bundle formation was also examined by electron microscopy after mixing 3 μM f-actin with various peptides at 120 μM for 10 min.

Circular Dichroism (CD) Spectra of Scruin–Calmodulin Complex and Calmodulin

CD was performed on an Aviv 62 DS spectrometer. Spectra of scruin–calmodulin complex at 4.4 μM and 4.4 μM calmodulin in 0.15 M NaCl and 3 mM Tris (pH 8.0) were recorded at 0°C in a 1-mm path-length cuvette. The temperature dependence of the CD signal was monitored at 215 nm for the scruin–calmodulin complex and 222 nm for calmodulin using a step size of 2°C, a 30-s signal averaging time, and a 2-min equilibration period.

RESULTS

Titration of the Reactive Cysteines in Scruin

Scruin contains 11 cysteine residues. If any cysteine residue is exposed to solvent, then the free thio groups should react with Ellman's reagent (Figure 1). We found that at a DTNB:scruin molar ratio of 1.5:1, an equivalent of 1.5 cysteine residues was modified by 30 min. However, at higher DTNB:scruin molar ratios (3:1 to 41:1), 2 mol of cysteine were modified within the same period but the reaction slowly approaches a maximum of 2.5 mol equivalents after 1 h. Because the solution of actin bundles is turbid, the reactive cysteines in the purified acrosomes could not be studied in spectrophotometric assays.

Inhibition of Actin Bundling Activity by Cysteine Modification

Because at least two to three cysteine residues were exposed to solvent, we tested whether modification of

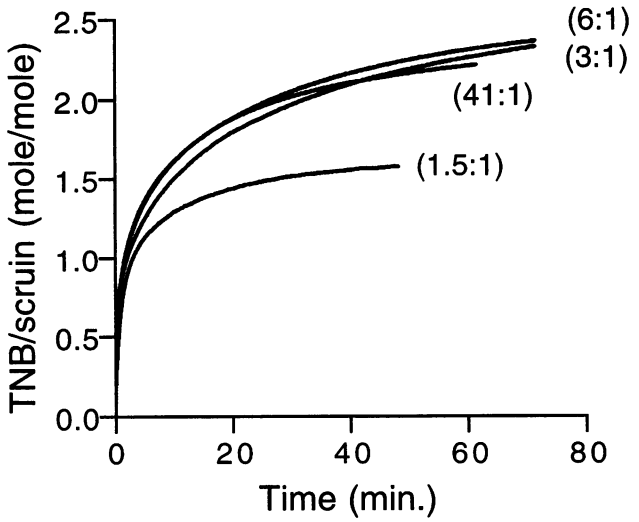

Figure 1. Time course of the DTNB reaction with scruin. Scruin was reacted with DTNB at DTNB:scruin molar ratios of 1.5:1, 3:1, 6:1, and 41:1, and the TNB product was measured.

these residues inhibited the actin-binding and cross-linking activity of scruin (Figure 2). In a high-speed pelleting assay, unmodified scruin cosedimented with f-actin (Figure 2A). However, less scruin was found in the pellets and more scruin remained in the supernatant if scruin was first labeled with the thiol-reactive dye 1,5-IAEDANS. Under conditions in which at least two equivalents of cysteine are modified (a dye:cysteine molar ratio of 4.1:1), more than 80% of the scruin remained in the supernatant (Figure 2B). Since the pellet assay cannot distinguish the actin bundling from the actin-binding activity of scruin (at high-speed sedimentation, actin filaments also pellet), the inhibition of actin bundling was confirmed by electron microscopy. In the presence of unmodified scruin (Figure 2C), actin was organized into prominent bundles. In contrast, no actin bundles were detected when scruin was modified by the dye (Figure 2D).

Cysteine modification could inhibit actin binding by an indirect mechanism, for example, by altering scruin conformation at a binding site. To test for this possibility, we confirmed that cysteine modification did not disrupt the folded conformation of scruin by partial proteolysis with trypsin. Under conditions in which scruin is cleaved into two domains (Sanders *et al.*, 1996), the digested products of the labeled and unla-

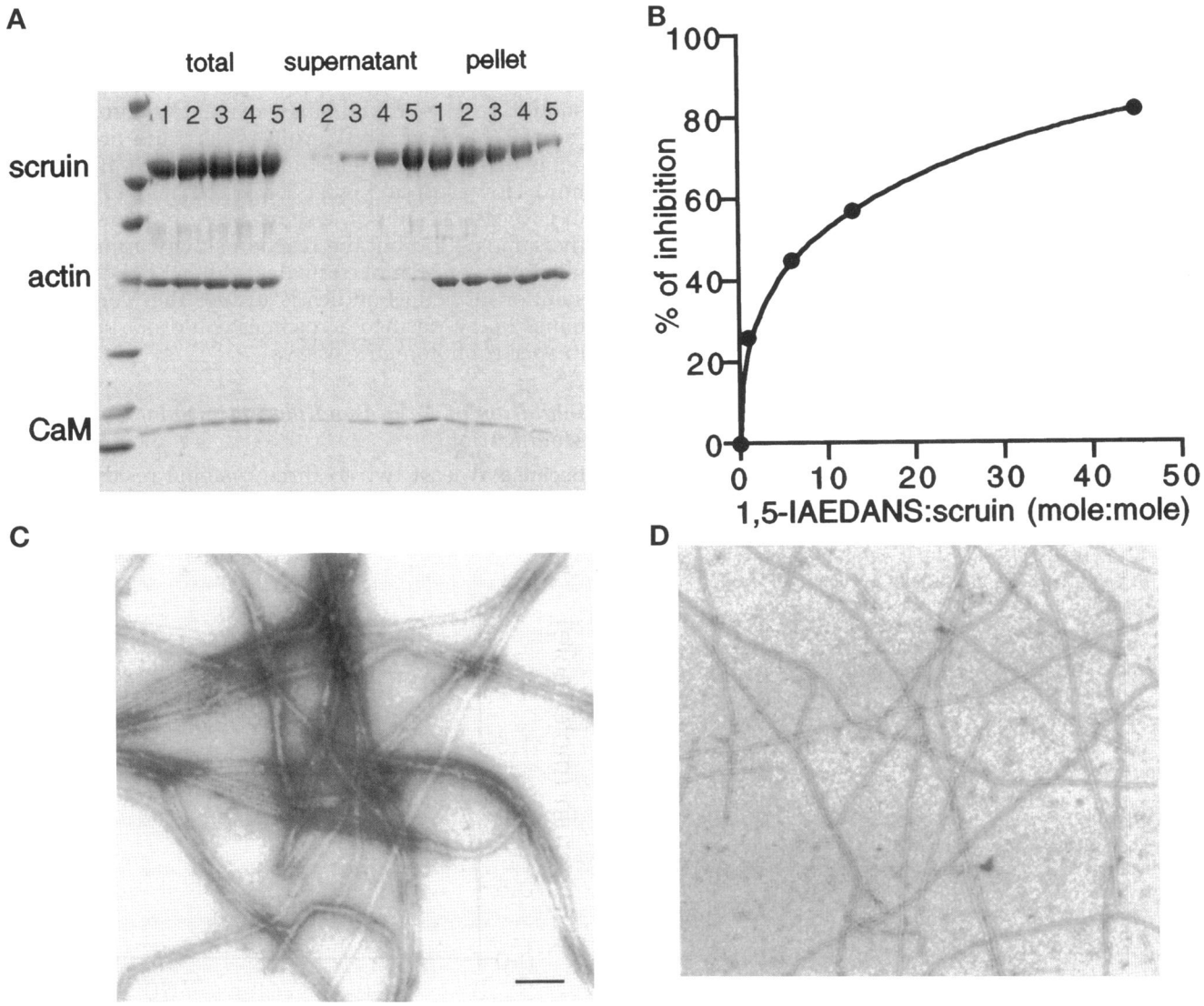

Figure 2. Inhibition of actin binding by cysteine modification of scruin. (A) Actin binding was measured by cosedimentation of 1,5-IAEDANS-modified scruin with actin filaments. Lanes 1–5 represent initial 1,5-IAEDANS:scruin molar ratios of 1:1, 6:1, 13:1, and 45:1. Equal aliquots of the sample before centrifugation (total) and the supernatant and pellet fractions were loaded in each lane. (B) Scruin in pellets shown in A is plotted as percentage of binding by unmodified scruin versus the molar ratio of 1,5-IAEDANS:scruin. (C and D) Electron micrograph of f-actin mixed with unmodified scruin (C) and modified scruin (D). Bar, 100 Å.

beled scruin protein were identical (our unpublished results). This suggests no significant conformation change in the labeled scruin.

Identification of the Reactive Cysteines in Scruin and in True Discharge

Because actin binding is inhibited when at least 2 mol of cysteine are modified, we used a combination of HPLC, mass spectrometry, and protein sequencing to identify the modified residues and determine the stoichiometry of labeling. In Figure 3, we compare the HPLC chromatographs of the trypsin-generated peptide maps of labeled free scruin (top) with that of scruin labeled in the true discharge (bottom). In isolated scruin, mass spectrometry and protein sequencing identified five reactive cysteines: C146, C333, C683, C837, and C900. At low dye:cysteine ratios of 1.2:1 (our unpublished results), two residues, C837 and C900, are labeled. At a 4.1:1 dye:cysteine ratio, three other cysteines, C146, C683, and C333, reacted with 1,5-IAEDANS but to lesser extents than C837 or C900.

When scruin is bound to actin in the true discharge, new cysteine residues can become exposed to solvent due to conformational changes while other residues can become buried at interfaces with actin or other scruin molecules. To test whether cysteine residues are indicators of scruin-binding sites or conformational changes, we determined the pattern and level of cysteine modification of scruin in the acrosomal process (Figure 3, bottom). The chromatographs show that the reactivity of all five cysteine residues was reduced and no new cysteines became modified. Two minor peaks that eluted at 73 min were contaminants in the true discharge sample. One residue, C333, was poorly reactive in scruin and was not labeled at all in the true discharge. However, of the two most reactive cysteines, C837 and C900, in isolated scruin, only one, C837, became unreactive to modification in the true discharge. Interestingly, no cysteine residues in actin, especially C374, was modified in scruin–actin complexes.

To determine the stoichiometry of cysteine modification, we quantified the amount of dye in each peak at different dye:cysteine ratios (Figure 4). At low dye:cysteine ratio, 1.2:1 (Figure 4A), C900 in scruin was 80% labeled, whereas other sites were labeled at trace levels. In an excess of dye, other sites became significantly modified, 40% labeling at C146 and C333, 85% labeling at C683, and 95% labeling at C837. In contrast, the overall reactivities of cysteines of scruin were decreased in the true discharge. The most reactive cysteine C900 was labeled to 40–50% at a dye:cysteine ratio of 4.1. The most significant change in reactivity was at C837. Its reactivity decreased from 100% in scruin to about 4% in the true discharge (Figure 4B).

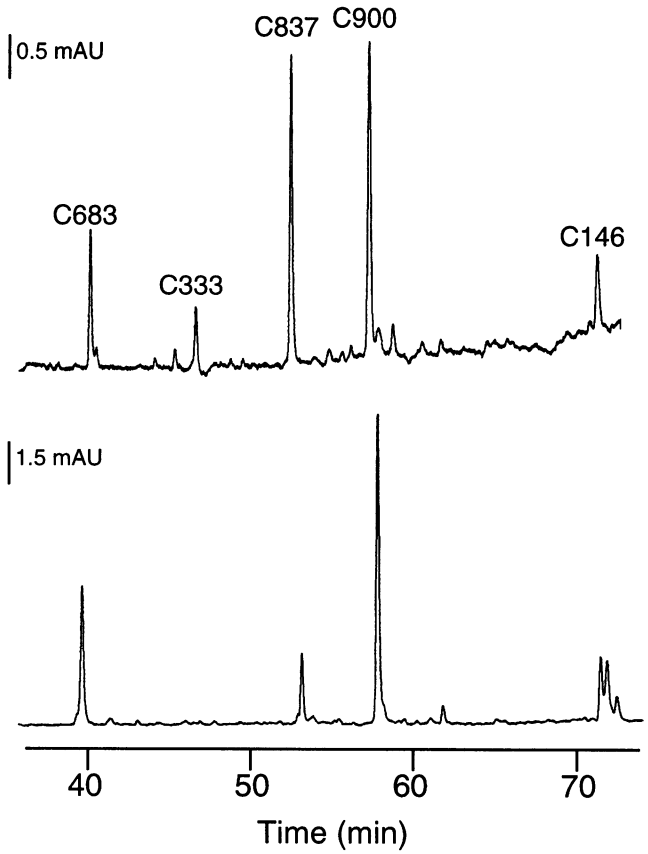

Figure 3. HPLC analysis of reactive cysteines. Scruin at 0.05 nmol (top) and true discharge at 0.3 nmol (bottom) reacted with 1,5-IAEDANS at a 45-fold molar excess were digested with trypsin and separated by reverse-phase HPLC. The dye-labeled peptides were identified by matrix-assisted laser desorption time-of-flight mass spectrometry and Edman chemical sequencing.

Assignment of the Cysteine Involved in the Actin Binding of Scruin

Because actin binding is almost completely inhibited when C837 and C900 are completely modified (Figures 2B and 4A), we examined whether one site is critical for actin binding by comparing the extent of labeling (Figure 4A) with the extent of actin binding (Figure 2B). The analysis (Figure 5) reveals that when 50% of the C900 was modified, 80% of the protein was able to bind actin. A better correlation between binding and extent of modification is seen with C837. When this site was 50% modified, actin-binding activity was reduced to 30% compared with that of the unmodified protein. Under these conditions, the other sites were not labeled by the dye and thus could not account for the inhibition of binding.

The analysis of Figure 5 assumes that cysteine modification causes total loss of actin binding. However, it may be that cysteine modification only decreases the scruin–actin-binding constant. In this

case, there would be no quantitative correlation between cysteine modification and inhibition of actin binding, making it difficult to distinguish between roles played by C900 and C837. However, when we consider the fact that C837 is virtually unmodifiable when scruin is bound to actin (Figure 3), it appears that C837, not C900, is involved in the scruin–actin interaction.

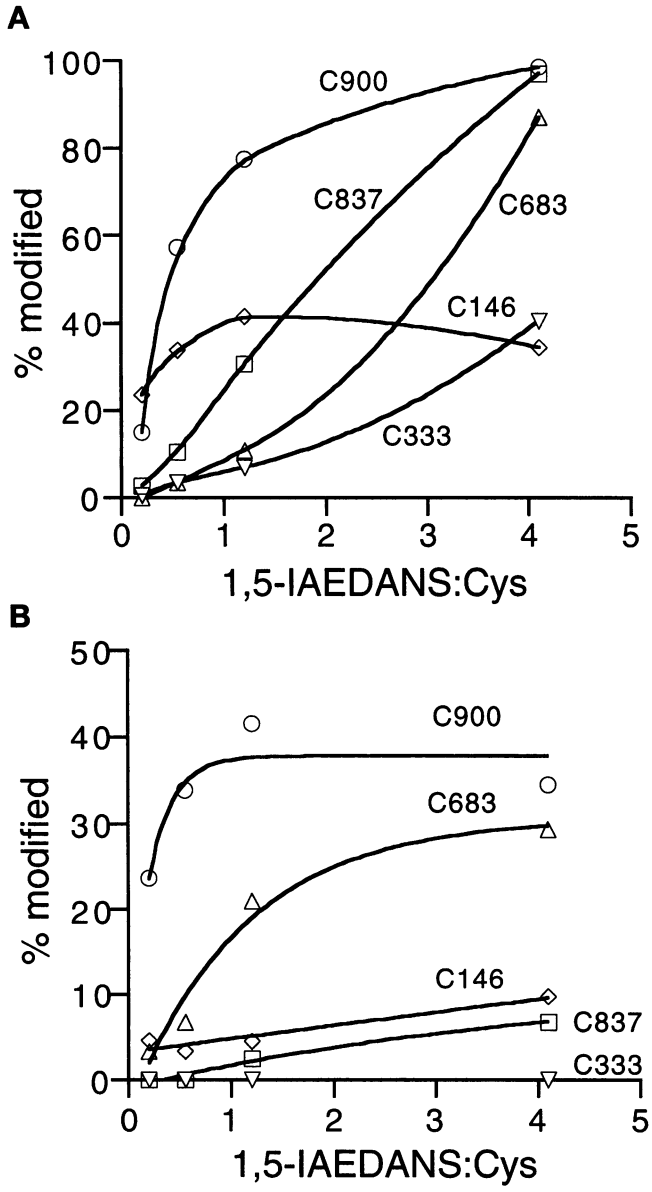

Figure 4. Relative reactivity of cysteine residues in scruin (A) and the true discharge (B). C900, ○; C837, □; C863, △; C333, ▽; C146, ◇. The amount of each modified cysteine was measured at different dye:cysteine molar ratios by HPLC and normalized to the input scruin concentrations.

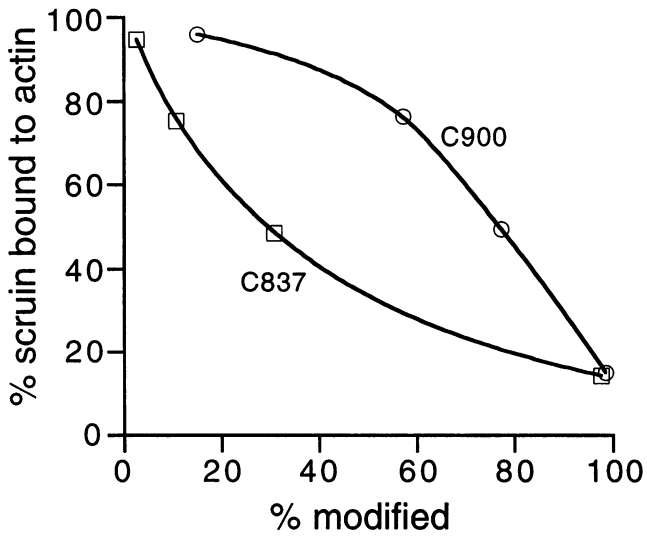

Figure 5. Correlation between actin binding and modification of C837 (□) and C900 (○). The binding data in Figure 2B and quantitation of reactive cysteines in Figure 4A were replotted to show the relative effect on actin binding by the two most reactive cysteines of scruin.

Actin-binding Activity of Peptide Models Containing C837

Chemical modification experiments suggested that C837 played a crucial role in binding f-actin. We studied the involvement of this residue in the scruin–actin interaction using a synthetic peptide that contained C837 and its flanking sequence. Since the affinity of peptides for f-actin is often very weak, we adopted a strategy used to enhance the apparent binding affinity of a peptide by forming peptide dimers through a disulfide linkage (de Arruda *et al.*, 1992). In this assay, actin-binding activity is detected by the presence of actin bundles. Figure 6 shows the results of light scattering when f-actin was mixed with the peptide dimers formed through a disulfide bond. M39, the peptide corresponding to residues 830–842 of scruin, cross-linked f-actin into bundles at concentrations >100 μM (Figure 6). No cross-links were detected at lower concentrations of peptide or in the presence of the reducing agent DTT. To investigate the role of cysteine at position 837 in peptide M39, we substituted cysteine with alanine and introduced a cysteine at the NH_2 or C terminus. Curiously, the actin-binding activity was dependent on the location of the disulfide bond. In comparison to the native peptide, actin-binding activity was higher when the peptide is dimerized at the C terminus (M39R4). Very little binding activity was detected when the disulfide bond was at the NH_2 terminus (M39R3) or in a control peptide (M39R2) with the same amino acid composition but whose sequence was randomized. These results were confirmed by electron microscopy with the peptides at

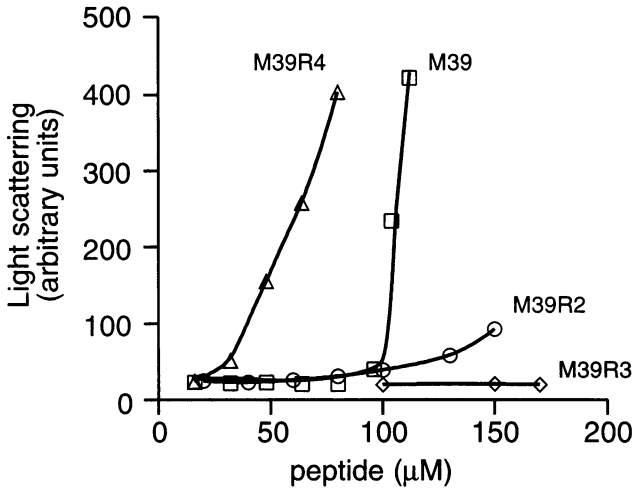

Figure 6. Actin bundling activities of synthetic peptides. The f-actin at 3 μM was mixed with various amounts of peptide in binding buffer [10 mM piperazine-*N*,*N*′-bis(2-ethanesulfonic acid), 50 mM NaCl, 1 mM $MgCl_2$, 0.1 mM ethylene glycol-bis(β-aminoethyl ether)-*N*,*N*,*N*′,*N*′-tetraacetic acid, 0.5 mM ATP, pH 7.0]. Peptides used are as follows: □, M39; ○, M39R2; ◇, M39R3; △, M39R4.

100 μM. Peptides M39 and M39R4 bundle actin, whereas M39R2 and M39R3 do not.

Secondary Structure Determination of Scruin

To interpret our chemical modification results, we must be able to map the modified sites onto a 3D structure. Since protein sequence analysis of scruin has predicted a predominantly β-strand secondary structure (Way *et al.*, 1995a), we tested this prediction with CD spectroscopy. A CD spectrum of scruin showed the protein contains predominantly β-strand secondary structure. However, because scruin is complexed with calmodulin in a 1:1 molar ratio, the CD spectrum of scruin alone was obtained by subtracting the calmodulin spectrum from that of the complex. This calculated difference spectrum assumes that the secondary structure of scruin is not significantly affected by calmodulin binding (Figure 7A). Deconvolution of the spectra using a computer program, PROSEC, estimated approximately 60% of β-strand secondary structure for scruin and a similar number for the scruin–calmodulin complex. Analysis of the CD spectrum for calmodulin produced 0% of β-strand structure, which agreed very well with the secondary structure of calmodulin (Chattopadhyaya *et al.*, 1992). To probe the stability of the protein, we monitored the presence of β-sheet structure during temperature scan from 0 to 95°C. The protein was stable up to 60°C, at which point it exhibited an abrupt transition to the unfolded state. The melting temperature (T_m) from folded to unfolded form for the scruin–calmodulin complex was 62°C (Figure 7B). A similar transition temperature was observed for pure calmodulin. The transition is also irreversible unlike calmodulin, which refolds upon lowering the temperature.

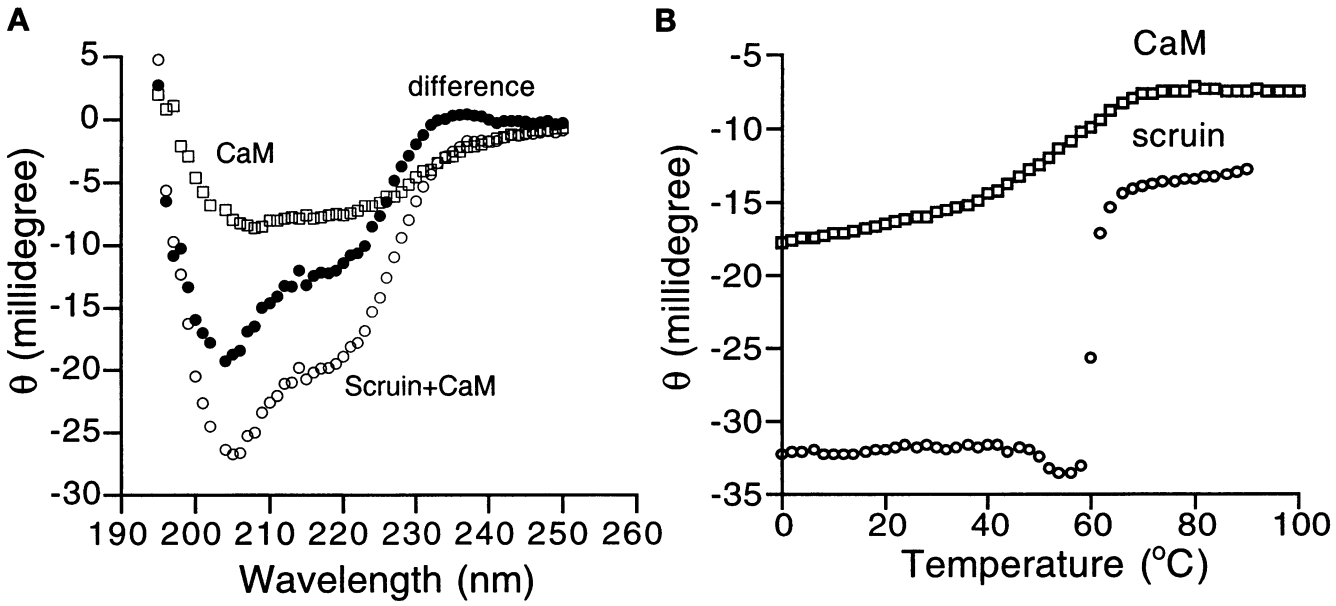

Figure 7. Secondary structure measurement and thermal stability of scruin. (A) CD spectra of the scruin–calmodulin complex (4.4 μM, ○), calmodulin (4.4 μM, □), and scruin (●) obtained by subtracting values for calmodulin (□) from values for the scruin–calmodulin complex (○). (B) Temperature dependence of the CD for the scruin–calmodulin complex at 215 nm (○) and for calmodulin at 222 nm (□).

DISCUSSION

The unactivated acrosome in the *Limulus* sperm resembles a coiled rope. During the acrosome reaction, the actin filaments untwist by 0.2 degree per subunit and the bundle uncoils and straightens (De Rosier *et al.*, 1982). This profound and dynamic change in actin filament structure and bundle organization must involve significant changes in the binding interactions between scruin and actin. To understand the mechanism and the driving force in the acrosome reaction, we need to identify how the three components of the actin bundle, actin, scruin, and calmodulin interact with each other and compare these interactions in the coiled and straightened acrosomes. Since the coiled actin bundle has not been isolated, our studies have focused on the activated acrosomal process, the true discharge. The results reported in this article probe the surface of scruin and identify sites that are exposed to solvent and also involved in actin binding. Furthermore, the reactive cysteine residues provide important information in fitting the scruin sequence to a structural model of the protein.

C837 Lies at an Actin-binding Interface

Chemical modification of cysteine residues is a classic approach to identify enzyme-active sites and protein-binding sites (Lundblad, 1991). In our studies, we have shown that one of two highly reactive cysteines, C837, is involved in actin binding. Three independent lines of evidence support this conclusion. First, modification of this cysteine closely correlates with the loss of actin-binding activity. Because scruin binds actin in a 1:1 stoichiometry, we should expect a 1:1 relationship between the extent of scruin inactivation with the extent of scruin modification. With other cysteine residues, either the stoichiometry of label is too low (C683) to account for 100% inhibition or too high (C900) to explain why the modified protein is still able to bind actin. Second, C837 is protected from modification when scruin is bound to actin in the acrosomal process. Although other residues also become less reactive, none except C837 is 100% reactive in the isolated state and virtually unreactive (4%) in the actin-bound state. This protection from chemical modification mimics what one would expect if C837 lies in the binding footprint of actin. Third, in our actin bundling assay with disulfide-bonded dimer peptides, we show that the sequence containing C837 binds actin filaments. Thus, we demonstrate in this report that C837 is exposed on the surface of the native protein and is located within an actin-binding site.

One caveat of our model is that the reduced reactivities at some sites may reflect scruin–scruin interactions that are necessary to form cross-links between filaments. Although scruin is bound to actin in a 1:1 stoichiometry, a subset of the scruin molecules will also interact with scruin on neighboring filaments. Because an actin filament is helical, some but not all scruin molecules are positioned to bind a neighboring filament. It is not possible to estimate the fraction of scruin molecules that form cross-linking complexes, although a conservative guess would be 20% based on studies of fascin cross-links in microvillar actin bundles by De Rosier and Edds (1980). Thus, we would expect that a fraction of the reactive cysteine residues would be similarly reduced in the stoichiometry of labeling.

Although C837 is at the binding interface, it probably does not interact directly with actin because replacement of cysteine with alanine in the peptide models does not inhibit binding. This observation may seem to contradict our chemical modification experiments. However, a simple explanation is that covalent attachment of 1,5-IAEDANS sterically hinders binding to surrounding residues. This is supported by one additional result. Labeling of cysteines with a smaller cysteine specific reagent, *N*-ethylmaleimide, also inhibited actin binding but to a lesser extent. Because the methyl side chain of alanine is approximately the same size as the cysteine thiol side chain, the substitution is not expected to inhibit binding.

If cysteine is not directly involved in binding, what other residues mediate actin binding? A clue to the answer lies in comparison of the sequences of the peptide variants and the location of the disulfide bond (Figure 6). When the disulfide bond is placed at the NH_2 terminus, binding is reduced. Placing the disulfide at the opposite end of the peptide generates the highest activity in the actin-binding peptide. In the wild-type sequence, the disulfide is located near the middle of the peptide. The corresponding peptide binds actin with an intermediate apparent affinity. Since binding activity decreases as the disulfide is moved toward the NH_2 terminus, we conclude that the actin-binding activity is localized to a region at or near the NH_2 terminus of the peptide.

Loops and a Model for the Topology of Scruin

Until a high-resolution structure is obtained, we can use the structures of related proteins and the pattern of cysteine reactivities to refine our model of scruin structure (Sanders *et al.*, 1996). Crucial to our model is that scruin belongs to a superfamily of proteins that include galactose oxidase (Ito *et al.*, 1994), neuraminidase (Varghese and Colman, 1991), and kelch (Bork and Doolittle, 1994). A diagnostic feature of the scruin sequence is the tandem repeat of a 50-amino acid sequence that contains widely spaced highly hydrophobic residues followed by conserved Gly-Gly and Trp-X residues. The 3D structure of several members of this family shows that each consensus repeat is a sheet of four antiparallel β-strands joined by loops

and turns of variable sizes and twisted like a β-blade. Typically, six or seven β-blades are arranged circularly. Recently, the β-propeller repeats were discovered in the 3D structure of the β-subunit of the heterotrimeric G protein, a protein that contains 40-amino acid sequence repeats characterized by conserved Gly-His and Trp-Asp residues (Wall *et al.*, 1995). This structural homology brings two large superfamilies, the WD-40 repeat proteins (Neer *et al.*, 1994) and the kelch repeat proteins, into one large β-propeller superfamily.

The proposed β-sheet secondary structure for scruin is supported by the CD analysis of the scruin–calmodulin complex. Deconvolution of the CD spectrum of the scruin–calmodulin complex revealed around 60% β-sheet structure for the complex. Since calmodulin lacks any β-structure, we assume that the β-sheet secondary structure in the complex is derived solely from scruin. The melting temperatures for the scruin–calmodulin complex and for calmodulin alone are similar, both around 62°C, which suggests that calmodulin binding does not alter structure. The sharp transition in denaturation of the scruin–calmodulin complex (within 4°C) indicates high cooperativity in the unfolding process. The cooperativity in unfolding can be explained by the model of the circularly arranged β-blades; as a few blades unfold, the protein completely denatures.

The first step in constructing a model is to determine where a repeat sequence begins and ends. Although we have aligned the scruin repeats to either the kelch family (Way *et al.*, 1995a) or WD-40 family of sequences (Way *et al.*, 1995b), our chemical modification data and a better understanding of the 3D structures suggest that scruin is more kelch-like. The most distinguishing feature of the known structures is that the innermost β-strand consists of small side chains and that the largest region between repeats should correspond to the chain linking adjacent repeats (strand 4 of one repeat to strand 1 of the next repeat). We determined that our fit of scruin to the WD-40 repeat in a previous article (Way *et al.*, 1995b) is unlikely because the region of sequence that connects neighboring repeats would correspond to a segment of sequence too short to span the minimum distance and large side chain amino acids would form the inner strand.

Once the "phase" of the sequence repeats is established, we can examine whether regions predicted to be exposed or buried contain reactive or unreactive cysteine residues. Based on a kelch-like repeat fitted to the β-propeller structure (Figure 8), all of the reactive cysteines except C900 occur in turns that connect adjacent β-strands or loops between β-propeller motifs. Furthermore, all of the reactive cysteines map to the same side of the motif (Figure 8). Peptide M39 corresponds to a loop that connects 5b with 6b. The unreactive cysteines except C373 are either in the turns

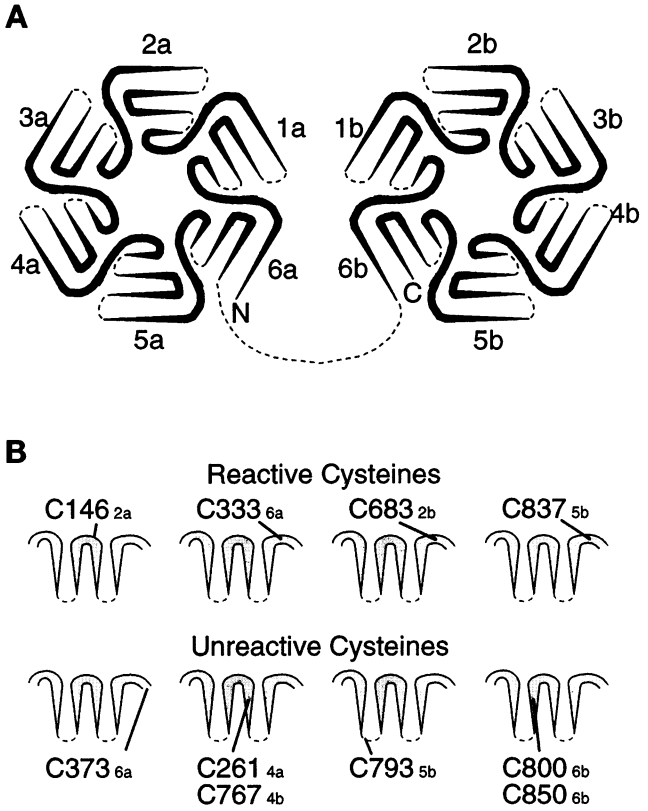

Figure 8. Schematic 3D model of scruin. (A) The N-terminal (1a–6a) and C-terminal (1b–6b) domains of scruin are arranged into structurally homologous β-propellers. The loops connecting two adjacent β-blades and the turns between the inner two β-strands face one side of the domain (heavy lines), whereas the turns between the innermost or the outermost β-strands lie on the opposite side of the domain (dot lines). (B) The schematic picture indicates that all of the reactive cysteines are located in the loops or turns on one side of the β-propeller, whereas the remaining cysteines lie predominantly in the β-sheets.

facing down or lie within the β-sheets and thus are directed toward the hydrophobic interior. Thus, the reactivities are completely consistent with their locations in the proposed model and provide a chemical justification of the model.

Structure and sequence homology between the N- and C-terminal domains lead to an assumption that similar actin-binding sites lie on the two domains. Because the turns and loops connecting adjacent β-blades provide the bulk of the exposed surface in β-propeller proteins, it is plausible that they form the actin-binding sites. We propose that loop regions on one face of scruin are involved in actin binding because their cysteines are less accessible to solvent when scruin is bound to actin. Furthermore, our experiments showed not only that modification of C837 in one putative loop region inhibits binding by native scruin but also that a peptide corresponding to the same loop sequence also binds actin outside the con-

text of a folded protein structure. Thus, we have narrowed an actin-binding site to include residues defined by the peptide models. However, more biochemical and structural studies are required to identify the binding residues. Widely spaced basic, acidic, and polar residues are thought to be important in binding actin for the villin headpiece (Doering and Matsudaira, 1996; Friederich *et al.*, 1992). Interestingly, a KQK is at the NH_2 terminus of peptide M39. These residues could mediate scruin binding to a conserved helix loop-strand on the surface of actin subdomains 1 and 3 (Schmid *et al.*, 1994). These sites form the region of actin that overlaps with density from scruin in EM reconstructions.

Two cysteines map to regions outside of the β-propeller domains. C373 is close to the calmodulin-binding neck region that connects the two β-propeller domains. C900 is in the C-terminal region outside the β-propeller domain. Currently, we are extending our EM studies with reconstructions of the actin bundle and higher resolution studies of the acrosomal filament. These studies (Sherman, Jakana, Schmidt, Sun, Footer, Matsudaira, and Chiu, unpublished results) will reveal how scruin interacts with neighboring filaments and the stoichiometry of their binding.

ACKNOWLEDGMENTS

We thank Mitchell Sanders for his help in the early stage of scruin purification and Ya-Huei Tu for technical assistance in electron microscopy. This work was supported by a grant from the National Institutes of Health (GM-52703).

REFERENCES

André, J. (1965). A propos d'une Leçon sar la limule. Ann. Fac. Sci. *26*, 27–38.

Bork, P., and Doolittle, R.F. (1994). *Drosophila* kelch motif is derived from a common enzyme fold. J. Mol. Biol. *236*, 1277–1282.

Chattopadhyaya, R., Meador, W.E., Means, A.R., and Quiocho, F.A. (1992). Calmodulin structure refined at 1.7-Å resolution. J. Mol. Biol. *228*, 1177–1192.

de Arruda, M.V., Bazari, H., Wallek, M., and Matsudaira, P. (1992). An actin footprint on villin: single site substitutions in a cluster of basic residues inhibit the actin severing but not capping activity of villin. J. Biol. Chem. *267*, 13079–13085.

De Rosier, D.J., and Edds, K.T. (1980). Evidence for fascin crosslinks between the actin filaments in coelomocyte filopodia. Exp. Cell Res. *126*, 490–494.

De Rosier, D.J., and Tilney, L.G. (1984). How to build a bend into an actin bundle. J. Mol. Biol. *175*, 57–73.

De Rosier, D.J., Tilney, L.G., Bonder, E.M., and Frankl, P. (1982). A change in twist of actin provides the force for the extension of the acrosomal process in *Limulus* sperm: the false-discharge reaction. J. Cell Biol. *93*, 324–337.

Doering, D.J., and Matsudaira, P. (1996). Cysteine scanning mutagenesis at 40 of 76 positions in villin headpiece maps the f-actin binding site and structural features of the domain. Biochemistry *35*, 12677–12685.

Friederich, E., Vancompernolle, K., Huet, C., Goethals, M., Finidori, J., Vandekerckhove, J., and Louvard, D. (1992). An actin-binding site containing a conserved motif of charged amino acid residues is essential for the morphogenic effect of villin. Cell *70*, 81–92.

Ito, N., Phillips, S.E., Yadav, K.D., and Knowles, P.F. (1994). Crystal structure of a free radical enzyme, galactose oxidase. J. Mol. Biol. *238*, 794–814.

Lundblad, R.L. (1991). The modification of cysteine. In: Chemical Reagents for Protein Modification, ed. R.L. Lundblad, 2nd ed., Boca Raton, FL: CRC Press, 59–93.

Neer, E.J., Schmidt, C.J., Nambudripad, R., and Smith, T.F. (1994). The ancient regulatory-protein family of WD-repeat proteins (published erratum appears in Nature *371*, 812, 1994). Nature *371*, 297–300.

Owen, C., and D. DeRosier. (1993). A 13-Å map of the actin-scruin filament from the limulus acrosomal process. J. Cell Biol. *123*, 337–344.

Sanders, M.C., Way, M., Sakai, J., and Matsudaira, P. (1996). Characterization of the actin cross-linking properties of the scruin-calmodulin complex from the acrosomal process of *Limulus* sperm. J. Biol. Chem. *271*, 2651–2657.

Schmid, M.F., Agris, J.M., Jakana, J., Matsudaira, P., and Chiu, W. (1994). Three-dimensional structure of a single filament in the *Limulus* acrosomal bundle: scruin binds to homologous helix-loop-beta motifs in actin. J. Cell Biol. *124*, 341–350.

Tilney, L.G. (1975). Actin filaments in the acrosomal reaction of *Limulus* sperm: motion generated by alterations in the packing of the filaments. J. Cell Biol. *64*, 289–310.

Varghese, J.N., and Colman, P.M. (1991). Three-dimensional structure of the neuraminidase of influenza virus A/Tokyo/3/67 at 2.2-Å resolution. J. Mol. Biol. *221*, 473–486.

Wall, M.A., Coleman, D.E., Lee, E., J.A. Iniguez-Lluhi, Posner, B.A., Gilman, A.G., and Sprang, S.R. (1995). The structure of the G protein heterotrimer Giα1β1γ2. Cell *83*, 1047–1058.

Way, M., Sanders, M., Chafel, M., Tu, Y., Knight, A., and Matsudaira, P. (1995b). b-Scruin, a homologue of the actin crosslinking protein scruin, is localized to the acrosomal vesicle of *Limulus* sperm. J. Cell Biol. *108*, 3155–3162.

Way, M., Sanders, M., Garcia, C., Sakai, J., and Matsudaira, P. (1995a). Sequence and domain organization of scruin, an actin-cross-linking protein in the acrosomal process of *Limulus* sperm. J. Cell Biol. *128*, 51–60.